The Wigner function in paraxial optics I. Matrix methods in Fourier optics

Roberto Ortega-Martínez*, Carlos J. Román-Moreno
Centro de Ciencias Aplicadas y Desarrollo Tecnológico, Universidad Nacional Autónoma de México, Apartado Postal 70–186, 04510 México, D.F., México
**roberto@aleph.cinstrum.unam.mx*

Ana Leonor Rivera
Centro de Investigación en Ingeniería y Ciencias Aplicadas, Universidad Autónoma del Estado de Morelos, Cuernavaca, Morelos, México

Recibido el 19 de noviembre de 2001; aceptado el 10 de junio de 2002

The paraxial regime of scalar wave optics has the same structure as non-relativistic quantum mechanics, with wavelength taking the place of the Planck constant. The Wigner function is a central tool to explore the phase space of a system; in optics, moreover, it can be produced by purely optical means. In this first part, we present a matrix-based formalism for the study of paraxial optical systems, and apply it to the description of a setup that, as will be seen in the second part, produces the Wigner function.

Keywords: Wave propagation; Fourier optics; space phase measurements.

El régimen parxial de la óptica ondulatoria escalar tiene la misma estructura que la mácanica cuántica no relativista, donde la longitud de onda juega el papel de la constante de Planck. La función de Wigner es una herramienta central para explorar el espacio fase de un sustema; además, en óptica, se puede producir con medios exclusivamente ópticos. En esta primera parte, presentamos un formalismo matricial para el estudio de los sistemas ópticos parxiales y lo aplicamos en la descripciópn de un arreglo, que como veremos en la segunda parte, produce la función de Wigner.

Descriptores: Propagación de ondas; óptica de Fourier; mediciones de fase espacial.

PACS: 42.25.Bs; 42.30.Kq; 42.50.Dv

1. Introduction

Since the invention of the laser, signal analysis performed by optical means has become a powerful tool, due to its parallelism and speed. For signals in time, the conjugate variable is the frequency, (*i.e.*, the color for light or the tone for sound). Optical signals in space, on the other hand, are often understood as the light distribution on the plane of a screen perpendicular to the main direction of propagation. The conjugate variable is now the spatial frequency at the screen (called the momentum), which gives information about the direction of propagation of the different (plane wave) components of the field. For laser signal processors, the range of directions is usually very narrow, so it is valid to describe these systems by using the paraxial approximation. Paraxial wave optics is mathematically identical to non-relativistic quantum mechanics, with the wavelength λ taking the place of Planck's constant h.

An intuitive description for a signal is given by the Wigner function [1], which lives in phase space (the abstract space of time/position and frequency/momentum). The Wigner function does not contain 'more' information than the signal itself, but displays both the signal and its Fourier transform, and is tightly constrained by its mathematical properties. In particular, it implicitly includes the essential Fourier/Heisenberg 'uncertainty' relation between the two canonically conjugate variables.

In each domain (space and time) the Wigner function of signals has been studied and applied since the early 1980s. Bartelt, Brenner and Lohmann [2] built (paraxial) optical devices to produce the (square of the) Wigner function of a 1-dim signal in the space domain as a 2-dim image on a photographic plate. In the time domain, the development has followed a different route: 'instantaneous frequency' analyzers of analogue acoustic or radio signals were produced with electronic resonators more than a century ago. In fact, the representation of music by notes on a pentagram is somehow akin to a Wigner function, since it jointly specifies time and frequency.

The purpose of this series of tutorial papers is to guide the reader from the wave equation to the methods of paraxial optics that will let them understand the device in Ref. 2 for the implementation of the Wigner function. The mathematical tool most convenient to describe (paraxial, geometric or wave) optics is the theory of 2×2 matrices. This is not an understatement, because the methods include the necessary integral transforms of wave optics including Fourier and Fresnel transforms, Gaussians, coherent states and diffusion phenomena. We dedicate the first article in this series to the presentation of a shortcut from the home base of the wave equation to the point where matrices are used to analyze the Brenner-Lohmann setup which produces the Wigner function with monochromatic light of arbitrary color. The second article will give several examples of paraxial régime of scalar waves optics described by the Wigner function, and will present experimental results of its implementation in the laboratory; as usual, various parameters needed adjustment, so understanding the effects of misalignments, rotation and

unfocusing on the Wigner function image will rely on the results of this manuscript.

This paper is organized in the following way: Section 2. starts with the wave equation and narrows the range of interest to the paraxial régime. Fresnel propagators and thin lenses are the building blocks of optical systems and their action is specified on wavefields of arbitrary color and phase. Gaussians of complex width are fundamental to paraxial optics; in Sec. 3 we succinctly derive some of their properties and use them to find the canonical transform kernel, labelled by a 2×2 matrix, that carries the action of every optical system. Section 4 examines the manifold of free-lens-free systems, which includes fractional Fourier transformers. Out of two of these, with crossed cylindrical lenses, the Brenner-Lohmann setup is prepared for the following paper. Connections and conclusions are summarized in section 5.

2. Global and paraxial wavefields

A *wavefield* $\Psi(\vec{q};t)$ (of position $\vec{q} \in \Re^3$ and time $t \in \Re$) is a complex solution of the wave equation

$$\left(\frac{\partial^2}{\partial q_x^2}+\frac{\partial^2}{\partial q_y^2}+\frac{\partial^2}{\partial q_z^2}\right)\Psi(\vec{q};t)=\frac{1}{c^2}\frac{\partial^2}{\partial t^2}\Psi(\vec{q};t), \quad (1)$$

whose Fourier transform exists (at most) as a distribution (we thus implicitly exclude evanescent or otherwise growing solutions). Here, *c* is the speed of light.

2.1. Fourier transform of a wavefield

The spatial Fourier transform of a wavefield $\Psi(\vec{q};t)$ is

$$\begin{aligned}\widetilde{\Psi}(\vec{k};t) &= (\mathcal{F}:\Psi)(\vec{k};t)\\ &= \frac{1}{(2\pi)^{3/2}}\int_{\Re^3} d\vec{q}\,\Psi(\vec{q};t)\,\exp(-i\vec{k}\cdot\vec{q}) \quad (2)\end{aligned}$$

of *wavenumber* $\vec{k} \in \Re^3$, whose time dependence is determined by the Fourier transform of Eq. (1),

$$\partial^2\widetilde{\Psi}(\vec{k};t)/\partial t^2 = -(ck)^2\widetilde{\Psi}(\vec{k};t),$$

with $k = |\vec{k}\,|$. This equation has two independent separable solutions labelled by $\tau \in \{+1,-1\}$:

$$\widetilde{\Psi}(\vec{k};t)=\sum_{\tau=\pm1}\widetilde{\Psi}_\tau(\vec{k})\,\exp(-i\tau kct), \quad (3)$$

where $k = |\vec{k}\,| \geq 0$. This ensures that by Fourier synthesis, we recover the original function as

$$\begin{aligned}\Psi(\vec{q};t) &= (\mathcal{F}^{-1}:\widetilde{\Psi})(\vec{q};t)\\ &= \frac{\sum_{\tau=\pm1}}{(2\pi)^{3/2}}\int_{\Re^3} d\vec{k}\,\widetilde{\Psi}_\tau(\vec{k})\,\exp[i(\vec{k}\cdot\vec{q}-\tau kct)], \quad (4)\end{aligned}$$

The wavefield is thus displayed as a generalized (*Dirac*) superposition of plane waves $\sim \exp[i(\vec{k}\cdot\vec{q}-\tau kct)]$, whose wavefronts (i.e. surfaces of constant value) are normal to $\vec{k}$ and advance with time in the direction $\tau\vec{k}$. The wavelength $\lambda = 2\pi/k > 0$ is bound to the time frequency $\nu = \tau kc \in \Re$ by the propagation speed c in the medium. When $\widetilde{\Psi}_\tau(\vec{k})$ has support on a single sphere of radius $|\vec{k}\,| = k_o$, we say that the wavefield is *monochromatic*.

2.2. Wavefields near to the optical axis

We now consider wavefields composed of plane waves whose wavenumber vectors $\vec{k}$ are all *near* to the axis of the optical apparatus, denoted the z-axis, lying inside a *small* cone of angle Θ. In the usual spherical coordinates $\vec{k}(k,\theta,\phi)$ the $+z$-direction is $\theta = 0$; the wavenumber vector field $\widetilde{\Psi}_\tau(\vec{k}\,)$, is assumed to have support on the caps $|\theta| < \Theta$ and $|\pi-\theta| < \Theta$. Each small spherical cap maps 1:1 on a disk neighborhood of the origin in one of the two planes $k_z = \pm k$, that we label $\sigma = \operatorname{sign} k_z \in \{+1,-1\}$. On each of these σ-planes, we indicate by

$$\mathbf{p}=\frac{1}{k}\begin{pmatrix}k_x\\k_y\end{pmatrix}=\begin{pmatrix}\sin\theta\cos\phi\\\sin\theta\sin\phi\end{pmatrix}, \quad (5)$$

the *momentum* 2-vector, which we also label by σ. Then, the following approximations of order 2 in θ hold:

$$\begin{aligned}\frac{\sqrt{k_x^2+k_y^2}}{|k_z|} &= \tan\theta \simeq \sin\theta = \frac{\sqrt{k_x^2+k_y^2}}{k}\\ &= |\mathbf{p}_\sigma| \simeq \begin{cases}\theta, & \sigma=+1,\\ \pi-\theta, & \sigma=-1;\end{cases} \quad (6)\end{aligned}$$

$$k_z = \sigma\sqrt{k^2-k_x^2-k_y^2} \simeq \sigma k(1-\tfrac{1}{2}\mathbf{p}_\sigma^2), \quad (7)$$

$$\begin{aligned}d\vec{k} &= dk_x\,dk_y\,dk_z = k^2\,dk\,\sin\theta\,d\theta\,d\phi\\ &\simeq \sigma k^2\,dk\,d\mathbf{p}_\sigma, \quad (8)\end{aligned}$$

$$\vec{k}\cdot\vec{q} \simeq k\,\mathbf{p}_\sigma\cdot\mathbf{q}+\sigma k(1-\tfrac{1}{2}\mathbf{p}_\sigma^2)\,q_z, \quad (9)$$

where $\mathbf{q} = (q_x, q_y)$. The right-hand sides will define the *paraxial* approximation of the wavefield, which we now proceed to develop.

In this approximation, we can rewrite the Fourier synthesis of the wavefield (4) in cartesian coordinates $\vec{q} = (q_x, q_y, q_z) = (\mathbf{q}, q_z)$, as

$$\begin{aligned}\Psi(\mathbf{q},q_z;t) \simeq \frac{\sum_{\sigma,\tau=\pm1}}{(2\pi)^{3/2}}&\int_0^\infty k^2\,dk\,e^{ik(\sigma q_z-\tau ct)}\\ &\times\int_\Theta d\mathbf{p}_\sigma\,\widetilde{\Psi}_\tau(\mathbf{p}_\sigma,k)\,e^{-i\frac{1}{2}\sigma k\mathbf{p}_\sigma^2 q_z}e^{ik\,\mathbf{p}_\sigma\cdot\mathbf{q}}, \quad (10)\end{aligned}$$

where $\widetilde{\Psi}_\tau(\mathbf{p}_\sigma,k) = \widetilde{\Psi}_\tau(\vec{k}\,)$. There are four summands in (10), two containing the factor $e^{\pm ik(q_z-ct)}$ in the integrand, and two with $e^{\pm ik(q_z+ct)}$. The wave equation is of second order in t, so of course there are two independent solutions, determined by the initial conditions and derivatives. In the analysis of the output wavefield of an optical system we are

interested only in the $\sigma = \tau$ terms, which advance 'forward' with $q_z = ct$, containing both $\vec{k}$ and $-\vec{k}$, and whose momentum projections $\mathbf{p}_\pm$ are antiparallel. Writing $\mathbf{p} = \sigma\mathbf{p}_\sigma$, we can *replace* the integral over $k \geq 0$ in (10) by an integral over the real line σk of $\widetilde{\Psi}_\tau(\mathbf{p}_\sigma, k) = \widetilde{\Psi}_\tau(\mathbf{p}, \sigma k)$ times the exponential factors, where no explicit σ is left. We thus have forward wavefields written as

$$\Psi(\mathbf{q}, q_z; t) \simeq \frac{1}{\sqrt{2\pi}} \int_{-\infty}^{\infty} dk\, e^{ik(q_z - ct)}\, \frac{k^2}{2\pi} \times \int_\Theta d\mathbf{p}\, \widetilde{\Psi}(\mathbf{p}, k)\, e^{-i\frac{1}{2}k\mathbf{p}^2 q_z} e^{ik\,\mathbf{p}\cdot\mathbf{q}}. \quad (11)$$

2.3. Monochromatic wavefields, Fresnel propagator

To use the tools of Fourier analysis in their simplest form, having assumed that in principle $\widetilde{\psi}(\mathbf{p}, k) \approx 0$ for $|\mathbf{p}| > \Theta$, we now *disregard* this restriction and replace the integral (11) by an integral over the unbound momentum plane $\mathbf{p} \in \Re^2$. The inner integral in (11) is then

$$\bar{\psi}(\mathbf{q}, q_z; k) = e^{ikq_z} \frac{k^2}{2\pi} \times \int_{\Re^2} d\mathbf{p}\, \widetilde{\Psi}(\mathbf{p}, k)\, e^{-i\frac{1}{2}k\mathbf{p}^2 q_z} e^{ik\,\mathbf{p}\cdot\mathbf{q}}, \quad (12)$$

and this defines the *monochromatic field* of wavenumber k, whose time dependence is simple,

$$\psi_k(\mathbf{q}, q_z; t) = \bar{\psi}(\mathbf{q}, q_z; k)\, \frac{e^{-ikct}}{\sqrt{2\pi}}, \quad (13)$$

and whose integral over $k \in \Re$ yields the generic field (11). On the $q_z = 0$ plane —called the *standard screen*— the Gaussian oscillating factor in (12) is unity and $\bar{\psi}(\mathbf{q}, 0; k)$ is the inverse Fourier transform of $\widetilde{\Psi}(\mathbf{p}; k)$ with respect to the first two arguments; there, we can invert the relation (12) to

$$\widetilde{\Psi}(\mathbf{p}; k) = \frac{1}{2\pi} \int_{\Re^2} d\mathbf{q}\, \bar{\psi}(\mathbf{q}, 0; k)\, e^{-ik\mathbf{p}\cdot\mathbf{q}}. \quad (14)$$

Reintroducing this in (12), and after an exchange of integrations, we find that the wavefield at q_z is the convolution

$$\bar{\psi}(\mathbf{q}, q_z; k) = \int_{\Re^2} d\mathbf{q}'\, F(\mathbf{q} - \mathbf{q}', q_z; k)\, \bar{\psi}(\mathbf{q}', 0; k) \quad (15)$$

$$= \Big(F(\circ, q_z; k) \;*\; \bar{\psi}(\circ, 0; k)\Big)(\mathbf{q}) \quad (16)$$

between the field on the standard screen, and the *Fresnel propagator*

$$F(\mathbf{q}, q_z; k) = e^{ikq_z} \left(\frac{k}{2\pi}\right)^2 \int_{\Re^2} d\mathbf{p}\, e^{-i\frac{1}{2}k\mathbf{p}^2 q_z} e^{ik\,\mathbf{p}\cdot\mathbf{q}} = e^{ikq_z}\, \frac{-ik}{2\pi q_z}\, e^{ik\mathbf{q}^2/2q_z}. \quad (17)$$

Equation (15) is a superposition of diverging waves (17) with continuous coefficients $\bar{\psi}(\mathbf{q}', 0; k)$, similar to Huygen's construction.

2.4. Forward polychromatic paraxial wavefields

After all the approximations we made, we *replace* the 'true' wavefield $\Psi(\vec{q}; t)$ in (4) by the integral over all wavenumbers of the monochromatic fields (12) to form the (forward) *polychromatic paraxial* field

$$\Psi(\mathbf{q}, q_z; t) = \frac{1}{\sqrt{2\pi}} \int_{\Re} dk\, \bar{\psi}(\mathbf{q}, q_z; k)\, e^{-ikct}. \quad (18)$$

This expression has very convenient properties under Fourier transformation and fit naturally into the Wigner function formalism developed for quantum mechanics. For short, we call Eq. (18) the *paraxial regime* of wave optics.

To determine the form which the wave equation adopts in the paraxial régime, we note first that for the monochromatic fields $\psi_k(\mathbf{q}, q_z; t)$ in (13), the sum of second partial derivatives with respect to q_x and q_y multiplies $\widetilde{\Psi}(\mathbf{p}, k)$ in (12) by the factor $-k^2\mathbf{p}^2$, while the ct-derivative multiplies it by $-ik$ and the q_z-derivative by $ik(1 - \frac{1}{2}\mathbf{p}^2)$. Therefore, time-dependent paraxial monochromatic wavefields satisfy

$$-\frac{1}{2k^2}\frac{\partial^2}{\partial\mathbf{q}^2}\psi_k(\vec{q}; t) = \frac{i}{k}\frac{\partial}{\partial\frac{1}{2}(q_z + ct)}\psi_k(\vec{q}; t),$$

$$\frac{\partial}{\partial\frac{1}{2}(q_z - ct)}\psi_k(\vec{q}; t) = ik\psi_k(\vec{q}; t). \quad (19)$$

The first equation resembles the time-dependent free Schrödinger equation of quantum mechanics for unit mass, with a 'time' variable $\frac{1}{2}(q_z + ct)$ and a 'Planck reduced constant' $\hbar \leftrightarrow k^{-1} = \lambda/2\pi$ given by the *reduced wavelength* of each monochromatic field component, while the second equation only specifies that the field is indeed monochromatic and moving forward. When $\psi_k(\vec{q}; t)$ is replaced from the second equation into the first, all k's cancel and the full wave equation (1) is reproduced for any polychromatic sum or integral (18) of independent monochromatic components. When we place ourselves on a screen moving along the z-axis with the speed of light by setting $q_z = ct$, we remain only with the first of Eqs. (19), which is a free Schrödinger equation for the wavefields $\psi_k(\mathbf{q}, q_z)$ on $\mathbf{q} \in \Re^2$, and evolves along q_z.

2.5. The curious geometry of the paraxial approximation

The paraxial approximation of optics entails a curious geometry, as we illustrate here. Consider, as shown in Fig. 1, a wavefield of monochromatic plane waves (of wavenumber $k = |\vec{k}| = 2\pi/\lambda$), crossing (at a small angle θ from the normal of) a screen, and sensed on the screen by modulus and phase (as an acoustic wavefield could be). On the screen appears a pattern of parallel wavelines with wavenumber $|\mathbf{k}| = k|\mathbf{p}| = k\sin\theta \leq k$. As we increase the wavefield angle θ, the wavelines on the screen come closer together, spaced by a diminishing wavelength $\lambda_\theta = 2\pi/k|\mathbf{p}| = \lambda\sec\theta$; the

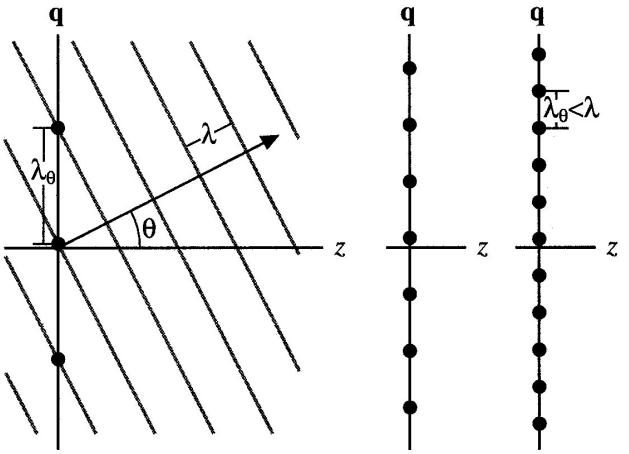

FIGURE 1. The curious geometry of the paraxial free propagation. A plane wavefield of wavelength λ falling on a screen at a 'small' angle θ shows wavelines on the screen, of transverse wavelength $\lambda_\theta = \lambda \csc\theta \geq \lambda$. Yet the paraxial régime 'foreshortens' angles so that λ_θ can be as small as close to λ.

minimal wavelength on the screen is λ for $\theta = \frac{1}{2}\pi$. But within the regime of 'paraxial geometry' we can increase $\theta \simeq |\mathbf{p}|$ beyond any bound, as if the foreshortening of λ_θ could continue down to zero. This is why paraxial optics, as quantum mechanics, can contemplate Dirac-δ's, or otherwise sharp (yet *monochromatic*) signals on its screen. With true wide-angle optics and in the absence of evanescent waves [Eq. (4)] one can define points on the screen only as sharply as the peak of a *sinc* function $\sin(k|\mathbf{q}|)/|\mathbf{q}|$ [3].

3. The Gaussian kernels of paraxial optics

Gaussian functions and their properties are germane to the paraxial régime of optics. They include the common bell shape, but also chirps whose local frequency increases linearly with time, serving both as a useful family of wavefields and as kernel for their transformations, as we shall now see.

3.1. Free propagation

In the previous Section, the approximation (7) of k_z from a sphere to a paraboloid was used to define the paraxial régime. In this régime, propagation of a wavefield from the standard screen to one at z along the optical axis, entails the transformation of the fields $\bar{\psi}(\mathbf{q}, z; k)$ of wavenumber k by an integral transform operator

$$[\mathcal{T}_z^k \bar{\psi}(\circ, 0; k)](\mathbf{q}) = \bar{\psi}(\mathbf{q}, z; k), \tag{20}$$

which acts by convolution (16) with the Fresnel propagation kernel (17). The latter consists of a phase factor e^{ikq_z}, times an oscillatory Gaussian function. We should expect that these operators are elements of a one-parameter group with identity $\mathcal{I}$:

$$\mathcal{T}_{z_1}^k \mathcal{T}_{z_2}^k = \mathcal{T}_{z_1+z_2}^k, \mathcal{T}_0^k = \mathcal{I}. \tag{21}$$

3.2. Thin lenses

Thin lenses are modelled conveniently by operators $\mathcal{L}$ of multiplication by oscillatory Gaussians: they must turn a plane wave into a spherical wave that converges to (or diverges from) a *focal point* at f along the optical z-axis, as shown in Fig. 2. On the reference plane (and for a 'small' angular spread), a converging spherical wave has phase $\sim \exp[-i\frac{1}{2}k(r-f)]$, where $r = \sqrt{\mathbf{q}^2 + f^2}$ is the radius to the focal point. The paraxial approximation is consistent with the consideration of lenses whose focal distance is very large in comparison with the transversal spread of the field, *i.e.*, $\mathbf{q}^2 \ll f^2$, the hypotenuse is $r - f \simeq \frac{1}{2}\mathbf{q}^2/f$, and the impressed phase is therefore $\exp(-i\frac{1}{2}k\mathbf{q}^2/f)$ on all incoming wavefields. In the paraxial model the *thin lens* approximation remains valid over all the plane $\mathbf{q} \in \Re^2$; in other words, pupils can grow infinitely wide and with no obliquity factor. We call $g = 1/f$ the *Gaussian power* of the lens, whose representing operator on fields of wavenumber k is

$$[\mathcal{L}_g^k \bar{\psi}(\circ, 0; k)](\mathbf{q}) = e^{-i\frac{1}{2}kg\,\mathbf{q}^2}\, \bar{\psi}(\mathbf{q}, 0; k) \tag{22}$$

A flat surface corresponds to the identity transformation $\mathcal{L}_0 = \mathcal{I}$ for $g = 0$. Convergent (convex) lenses are characterized by $g > 0$, and divergent (concave) ones by $g < 0$. An x-cylindrical lens $\mathcal{L}_{g_x,0}$ acts on the x-coordinate, multiplying the wavefield by $\exp(-i\frac{1}{2}kg_x q_x^2)$, and is flat in the y-direction. Similarly, a y-cylindrical lens $\mathcal{L}_{0,g_y}$ acts on the y-coordinate multiplying by $\exp(-i\frac{1}{2}kg_y q_y^2)$. The general *astigmatic* lens has in this exponent the quadratic form $\mathbf{q}\cdot\mathbf{g}\,\mathbf{q}$, with a symmetric 2×2 Gaussian power matrix $\mathbf{g}$; the lens is brought to its principal axes by rotating it around the optical axis; and there, the Gaussian power matrix is diagonal $\mathbf{g} = \mathrm{diag}\,(g_x, g_y)$. The set of astigmatic lens operators which generalize (22) also form a group [(21)] whose elements are symmetric matrices $\mathbf{g}$ and whose composition is their sum:

$$\mathcal{L}_{\mathbf{g}_1}^k \mathcal{L}_{\mathbf{g}_2}^k = \mathcal{L}_{\mathbf{g}_1+\mathbf{g}_2}^k, \mathcal{L}_{\mathbf{0}}^k = \mathcal{I}. \tag{23}$$

One-parameter subgroups of lenses are, for example, those characterized by $\mathbf{g} = g\mathbf{1}$ as *axis-symmetric* (*i.e.*, those which are invariant under rotations around the optical axis), and aligned cylindrical lenses $\mathbf{g} = \mathrm{diag}\,(g_x, 0)$, etc.

Three-dimensional paraxial optical systems, built out of paraxial free propagation and thin lenses, can be represented by 4×4 matrices of a certain type (*symplectic* matrices [4]) and form a 10-parameter group. In the paraxial régime moreover, there is a straightforward (and rather subtle) correspondence between geometric and wave optics, and between optics and mechanics of quadratic potentials (both classical and quantum) such as the free particle, the harmonic and the repulsive oscillators [5]). In this exposition, however, we shall

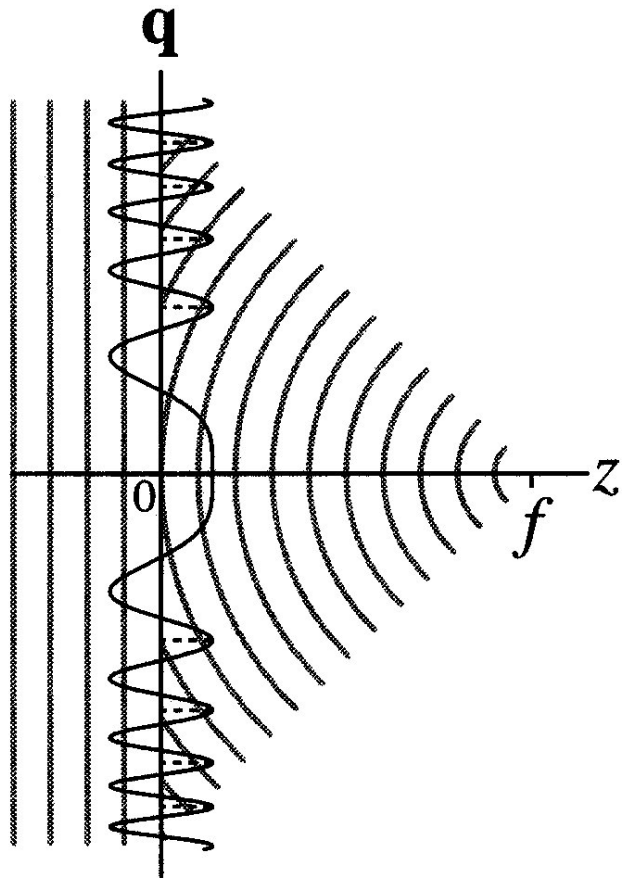

FIGURE 2. An ideal thin convex lens turns a plane wavefield into a convergent spherical one, multiplying by a phase factor. In the curious paraxial geometry, the spheres are approximated by osculating paraboloids and there is no pupil to restrict rays, nor obliquity factor.

be interested in a subset of systems composed of cylindrical lenses, all aligned on the x- or on the y-axes; and free propagation, which is axis-symmetric. Such systems are *separable* in x–y cartesian coordinates, so it is necessary to study lenses and free flights only on a single screen coordinate, as in a two-dimensional optical world.

3.3. Gaussian functions

As we saw above, both free-flight and lens transformations involve complex Gaussians, so we shall proceed now to gather their relevant properties for intensive use. We shall write the *Gaussian* function with the notation

$$G_\omega(q) = \frac{1}{\sqrt{2\pi\omega}}\, e^{-q^2/2\omega}, \qquad \mathrm{Re}\,\omega \geq 0, \quad \omega \neq 0, \quad (24)$$

where ω is a (complex) parameter loosely referred to here as the Gaussian's *width*. (Strictly speaking, the width is $\sqrt{\omega}$.) The theory of heat diffusion is well served by Gaussian 'bell' functions of real width $\omega > 0$ (proportional to *time*), and normalized such that

$$\int_{\Re} G_\omega(q)\, dq = 1, \qquad \mathrm{Re}\,\omega > 0. \qquad (25)$$

Now the Fresnel transform (17) contains Gaussians of pure imaginary width $\omega = -iq_z/k$, while the lens phase factor (22) multiplies with a Gaussian of width $\omega = -i/gk$. One may extend all formula to the limit $\mathrm{Re}\,\omega \to 0^+$ as long as integrals are performed in company with well-behaved square-integrable functions. This is the *weak* extension of functions that includes Dirac δ's as limit points of sequences of Gaussians.

The complex-ω Gaussian (24), shown in Fig. 3, is a two-valued function due to the square root of ω in the normalization factor. For the Fresnel propagator (17) one must specify that '$-i$' is $e^{-i\pi/2}$ (and not $e^{+3i\pi/2}$), because the normalization integral (25) exists only when we approach the imaginary-ω axis from the complex right half-plane. (The origin of this bivaluation is deeper: it relates to the *metaplectic sign* that underlies linear canonical transformations in paraxial geometric and wave optics.) When $|\omega| \to 0$ from the right half-plane, Eq. (25) implies that the Gaussian converges weakly to the Dirac $\delta(q)$; thus the limit $q_z \to 0^+$ of the Fresnel transform (15) is the identity transformation.

3.4. Fourier transform, convolution and product of Gaussians

A fundamental property of Gaussians is that the Fourier transform of $G_\omega(q)$ is also a Gaussian, albeit rescaled and of inverse width:

$$\widetilde{G}_\omega(q) = (\mathcal{F}\, G_\omega)(q) = \frac{1}{\sqrt{2\pi}} \int_{\Re} dq'\, G_\omega(q')\, e^{-iqq'}$$
$$= \frac{1}{\sqrt{\omega}}\, G_{1/\omega}(q), \qquad (26)$$

for $\mathrm{Re}\,\omega \geq 0$, $\omega \neq 0$. Since the product of exponentials corresponds to the sum of exponents, the product of two Gaussians (24) is a Gaussian whose width is the harmonic sum of the two widths:

$$G_{\omega'} \cdot G_{\omega''} = \sqrt{\frac{\omega}{2\pi\omega'\omega''}}\, G_\omega, \qquad \frac{1}{\omega} = \frac{1}{\omega'} + \frac{1}{\omega''}. \quad (27)$$

The Fourier transforms of (27) and (26) lead to the conclusion that the convolution of two Gaussians is a Gaussian with the sum of widths,

$$G_{\omega'} \ * \ G_{\omega''} = G_\omega, \qquad \omega = \omega' + \omega''. \qquad (28)$$

Thus, the concatenation of two free propagations (21) sums the displacements because the Fresnel propagators (15)–(17) convolute properly on the wavefields. Now, when the wavefield at a screen is itself a Gaussian bell of width ω ($\mathrm{Re}\,\omega > 0$), Eq. (28) shows that its width on a screen displaced by $z \in \Re$ will be $\omega(z) = \omega + iz/k$. Similarly, due to (27), a Gaussian wavefunction of complex width ω falling on one side of a thin lens of focal distance f turns into another Gaussian of width $1/\omega' = 1/\omega + i\frac{1}{2}gk$. The complex width parameter of Gaussians in optics remains thus in the right

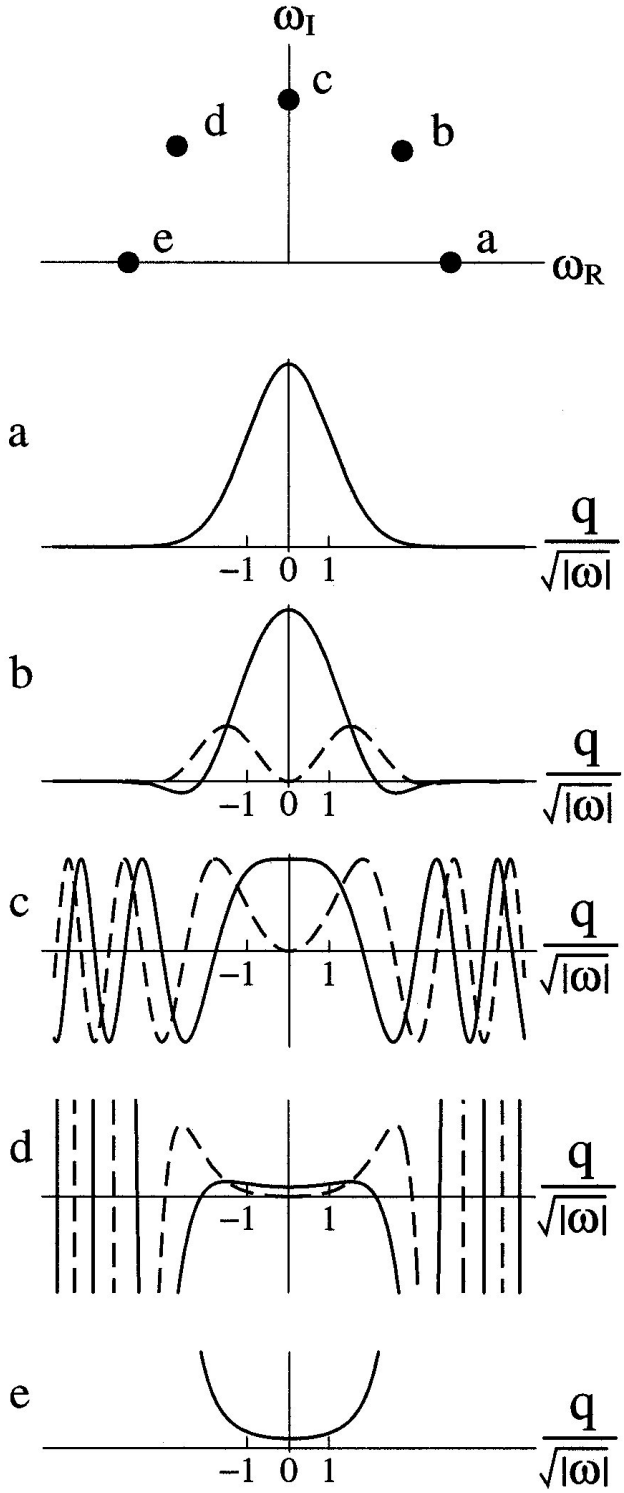

FIGURE 3. Growing, oscillating and bell-Gaussian functions for various values of its width in the complex plane.

half-plane. Lastly, note that due to the self-reproducing property of Gaussians under Fourier transformation (26), it follows that the free propagation and lens operators are Fourier conjugates of each other.

3.5. Optical elements act through canonical transforms

The transformations of two-dimensional monochromatic wavefields under the paraxial optical elements of propagation (16)–(17) and thin lenses (22), and also the Fourier transform (14) for wavenumber k, can be written most compactly using the *canonical transform* operators [6, 7] labelled by 2×2 matrices:

$$(\mathcal{T}_z\,\bar{\psi})(q;k) = e^{ikq_z}\int_{\Re^2} dq'\,G_{iz/k}(q-q')\,\bar{\psi}(q';k) \quad (29)$$

$$(\mathcal{L}_g\,\bar{\psi})(q;k) = \sqrt{\frac{2\pi}{ikg}}G_{1/ikg}(q)\,\bar{\psi}(q;k) = \left[\mathcal{C}\begin{pmatrix} 1 & 0 \\ -kg & 1 \end{pmatrix}\bar{\psi}\right](q;k), \quad (30)$$

$$(\mathcal{F}\,\bar{\psi})(q;k) = \frac{k}{\sqrt{2\pi}}\int_{\Re^2} dq'\,e^{-ik^2\,q\,q'}\,\bar{\psi}(q';k) = e^{i\pi/4}\left[\mathcal{C}\begin{pmatrix} 0 & 1/k^2 \\ -k^2 & 0 \end{pmatrix}\bar{\psi}\right](q;k). \quad (31)$$

In paraxial geometric optics [4], these operators act on the classical coordinates of position q and momentum $p = \sin\theta \simeq \theta$ of a ray through (inverse) matrix multiplication:

$$\mathcal{C}(\mathbf{M}) : \begin{pmatrix} q \\ p \end{pmatrix} = \mathbf{M}^{-1}\begin{pmatrix} q \\ p \end{pmatrix},\ \mathbf{M} = \begin{pmatrix} a & b \\ c & d \end{pmatrix}, \quad (32)$$

which must be of unit determinant, $\det\mathbf{M} = ad - bc = 1$, to satisfy symplecticity (conservation of rays).

In Fourier wave optics, the canonical operators $\mathcal{C}(\mathbf{M})$ act unitarily on square-integrable functions of the real line $f(q)$ through integral transforms, as

$$[\mathcal{C}(\mathbf{M})\,f](q) = \int_{\Re} dq'\,C_{\mathbf{M}}(q,q')\,f(q'), \quad (33)$$

with the Moshinsky–Quesne [6] integral kernel $C_{\mathbf{M}}(q,q')$ characterized by the matrix $\mathbf{M}$. From Eqs. (29–31) follows the generic form of this integral kernel:

$$C\begin{pmatrix} a & b \\ c & d \end{pmatrix}(q,q') = \frac{1}{\sqrt{2\pi i\,b}}\,\exp i \times\left(\frac{a}{2b}q'^2 - \frac{1}{b}q\,q' + \frac{d}{2b}q^2\right), \quad (34)$$

where the phase of i is understood to be $\frac{1}{2}\pi$. This includes properly the cases (29) and (31), while for the lens (30), the apparently singular limit $b \to 0$ can be evaluated using the stationary phase method [8, 11] and shown to be a weak convergence to an *imager* transform

$$\left[\mathcal{C}\begin{pmatrix} a & 0 \\ c & 1/a \end{pmatrix} f\right](q) = \frac{1}{\sqrt{a}}\exp\left(i\frac{cq^2}{2a}\right)\,f\left(\frac{q}{a}\right). \quad (35)$$

The parameters a, b, c, d may be complex, but absolute integrability demands that $\mathrm{Im}(a/b) \geq 0$. In particular, complex Gaussians (24) are canonical transforms of the Dirac δ_{q_o}

at the point q_o:

$$G_\omega(q-q_o) = \frac{e^{-(q-q_o)^2/2\omega}}{\sqrt{2\pi\omega}} = \left[\mathcal{C}\begin{pmatrix} 1 & -i\omega \\ 0 & 1 \end{pmatrix}\delta_{q_o}\right](q). \quad (36)$$

3.6. Composition of canonical transforms

A most useful property of the canonical transform operators and kernels is that they compose as their matrices multiply. Namely, when

$$\mathbf{M}_1\mathbf{M}_2 = \begin{pmatrix} a_1 & b_1 \\ c_1 & d_1 \end{pmatrix}\begin{pmatrix} a_2 & b_2 \\ c_2 & d_2 \end{pmatrix} = \begin{pmatrix} a_1a_2+b_1c_2 & a_1b_2+b_1d_2 \\ c_1a_2+d_1c_2 & c_1b_2+d_1d_2 \end{pmatrix} = \mathbf{M}_{12}, \quad (37)$$

the integral transform kernels satisfy [6, 7]

$$\int_{\Re} dq'\, C_{\mathbf{M}_1}(q,q')\, C_{\mathbf{M}_2}(q',q'') = \mu\Big(\frac{b_{21}}{b_1\, b_2}\Big)\, C_{\mathbf{M}_{12}}(q,q''), \quad (38)$$

with the *metaplectic sign* $\mu(w) \in \{+1,-1\}$ which is found when the complex integration is deformed carefully [7]. This $\mu(w)$ is $+1$ when w is in the closure of the first complex quadrant (including the positive real and positive imaginary boundaries), and -1 when w is in the third quadrant (including negative real and negative imaginary boundaries). Canonical integral transforms are a 2:1 cover of the group of 2×2 matrices of unit determinant, and *represent* the action of paraxial optical elements on paraxial wavefields.

3.7. Canonical transforms of Gaussian functions

Using (36) and (38) we can determine in closed form, and with only 2×2 matrix algebra, the transformations undergone by the width and center of Gaussian beams under generic paraxial optical systems. The generic canonical transform of the Gaussian (36) can be expressed as the kernel (34) through

$$\left[\mathcal{C}\begin{pmatrix} a & b \\ c & d \end{pmatrix} G_{\omega(\circ-q_o)}\right](q) = \left[\mathcal{C}\begin{pmatrix} a & b \\ c & d \end{pmatrix}\mathcal{C}\begin{pmatrix} 1 & -i\omega \\ 0 & 1 \end{pmatrix}\delta_{q_o}\right](q) = \mathcal{C}\begin{pmatrix} a & b-ia\omega \\ c & d-ic\omega \end{pmatrix}(q,q_o) \quad (39)$$

Now, in the opposite order for right- and left-triangular matrices, the result again is a Gaussian with a new width ω', a formal rescaled center $q'_o = \alpha q$, and a quadratic phase factor:

$$\left[\mathcal{C}\begin{pmatrix} 1 & -i\omega' \\ 0 & 1 \end{pmatrix}\mathcal{C}\begin{pmatrix} \alpha & 0 \\ c & \alpha^{-1} \end{pmatrix}\delta_{q_o}\right](q) = \sqrt{\alpha}\, e^{ic\alpha q_o^2/2}\left[\mathcal{C}\begin{pmatrix} 1 & -i\omega' \\ 0 & 1 \end{pmatrix}\delta_{\alpha q_o}\right](q) = \sqrt{\alpha}\, e^{ic\alpha q_o^2/2}\, G_{\omega'}(q-\alpha q_o). \quad (40)$$

We performed the first transform using (35) and rescaled $\delta(q/\alpha - q_o) = \alpha\,\delta(q-\alpha q_o)$; this is valid even though α is complex [for $\mathrm{Re}(\alpha^2) > 0$] as can be shown from

$$G_\omega(q/\alpha) = \alpha\, G_{\omega\alpha^2}(q), \quad (41)$$

in the limit when $\omega \to 0$. The product of the matrices in Eqs. (39) and (40) determines then the width and center of the Gaussian emerging at the end of the system $\mathbf{M}$:

$$\omega' = \frac{a\omega+ib}{d-ic\omega}, \qquad \alpha = \frac{1}{d-icw}. \quad (42)$$

The properties of Gaussians under canonical transforms will be used in the next article to compute the transformations of Gaussian beams under paraxial optical systems.

4. The free–lens–free configuration

As we said above, canonical transforms have the fundamental property of composing as their matrices multiply. If the optical elements are placed along the workbench from left to right, the corresponding operators must be ordered from right to left. It turns out that one can build a fair variety of optical systems with a single thin lens between a plane object at $z = 0$ and a screen at $z \in \Re$.

4.1. FLF imager systems

Two free propagation operators (29) by z_1 and z_2, on both sides of a thin lens (30) of power g, are shown in Fig. 4, and called the FLF configuration. When a forward monochromatic wavefield $\bar\psi(q;k)$ (the 'object') comes from the left, the wavefield at the screen z will be transformed through

$$\mathcal{S}\bar\psi(q;k) = (\mathcal{T}_{z_2}\mathcal{L}_g\mathcal{T}_{z_1}\bar\psi)(q;k) = e^{ik(z_1+z_2)}\left[\mathcal{C}\begin{pmatrix} 1 & z_2/k \\ 0 & 1 \end{pmatrix}\mathcal{C}\begin{pmatrix} 1 & 0 \\ -kg & 1 \end{pmatrix}\mathcal{C}\begin{pmatrix} 1 & z_1/k \\ 0 & 1 \end{pmatrix}\bar\psi\right](q;k) = e^{ik(z_1+z_2)}\left[\mathcal{C}\begin{pmatrix} 1-gz_2 & (z_1+z_2-z_1gz_2)/k \\ -kg & 1-z_1g \end{pmatrix}\bar\psi\right](q;k). \quad (43)$$

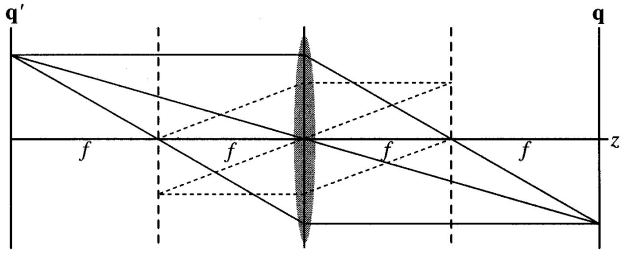

FIGURE 4. The free-lens–free configuration between the initial and final screen lines; the power of the lens is fixed but the free propagation intervals are variable. The system is an imager between the continuous lines (where the focal condition holds), a Fourier transformer between the dashed lines (where the Fourier condition holds), and a fractional Fourier transformer elsewhere.

This one-lens paraxial system will produce *images* when the 1–2 matrix element in the right-hand side of (43) is zero, because then Eq. (35) shows that the system maps the object $f(q)$ onto an image $\sim f(q/a)$ with at most a quadratic phase (leading to the same intensity distribution). An imager satisfies the

focal condition:

$$\frac{1}{z_1}+\frac{1}{z_2}=\frac{1}{f}=g, \quad \textit{i.e.},$$
$$\mathcal{C}\begin{pmatrix} 1-z_1 g & 0 \\ kg & 1-gz_2 \end{pmatrix}, \quad (44)$$

where the 1–1 element, $a=(1-z_1 g)^{-1}=1-gz_2=d^{-1}$, is the *magnification* factor. When this is negative, the image is inverted. We choose a *symmetric* FLF system by demanding $z_1=z_2$, and find from (44) that both the object and image lines lie at $z=\pm 2f$ from the lens; this is twice the focal distance.

4.2. Fourier and fractional Fourier transformers

The FLF one-lens configuration is an *inverse Fourier transformer* when the matrix in (43) is antidiagonal, as it is in (31), *i.e.*, when $1-z_1 g=0=1-gz_2$. A Fourier transformer satisfies the

Fourier condition:

$$z_1=z_2=f=\frac{1}{g}, \quad \textit{i.e.}, \quad \mathcal{C}\begin{pmatrix} 0 & 1/kg \\ -kg & 0 \end{pmatrix}. \quad (45)$$

The transform is (31) when $k=g$. This is also a symmetric FLF configuration where the object and image lines lie at the focal points of the lens: $z=\pm f$. A monochromatic wavefield $\bar{\psi}(q;k)$ at the former becomes $e^{-i\pi/4}\,e^{2ifk}\,(\mathcal{F}^{-1}\,\bar{\psi})(q;k)$ at the latter [Eq. (31)]; the phase $2fk$ comes from free flight over a total distance $2f$, which is in the first factor of the Fresnel propagator (17) and the canonical transform in (29).

Beside these two distinguished conjugate screens (see Fig. 4), the symmetric FLF configuration

$$\begin{pmatrix} 1-zg & z(2-zg)/k \\ -kg & 1-zg \end{pmatrix} = \begin{pmatrix} \cos\frac{1}{2}\pi\alpha & k^{-2}\sin\frac{1}{2}\pi\alpha \\ -k^2\sin\frac{1}{2}\pi\alpha & \cos\frac{1}{2}\pi\alpha \end{pmatrix} \quad (46)$$

provides the *fractional* power $-\alpha$ of the Fourier transform [9],

$$(\mathcal{F}^{\alpha}f)(q;k)=\frac{k\exp\Big[-i\frac{\pi}{2}\Big(\frac{1}{2}-\alpha \bmod 2\Big)\Big]}{\sqrt{2\pi|\sin\frac{1}{2}\pi\alpha|}} \times\int_{\Re}dq'\,\exp ik^2\Big(\tfrac{1}{2}(q^2+q'^2)\cot\tfrac{1}{2}\pi\alpha - qq'\csc\tfrac{1}{2}\pi\alpha\, qq'\Big)\,f(q';k). \quad (47)$$

For $\alpha=1$, (46)–(47) lead to the usual Fourier transform (45). The canonical transform operators (47) also form a group: $\mathcal{F}^{\alpha_1}\mathcal{F}^{\alpha_2}=\mathcal{F}^{\alpha_1+\alpha_2}$, and $\mathcal{F}^0=\mathcal{F}^4=1$ (*with* the aforementioned phase). For a given α, the FLF parameters are then $g=k\sin\frac{1}{2}\pi\alpha$ and $z=(\csc\frac{1}{2}\pi\alpha-\cot\frac{1}{2}\pi\alpha)/k>0$; both are finite for $0>\alpha>2$, the lower limit is the trivial identity transform with coincident input and output screens, while the upper limit blows up with $z\to\infty$. Imaging systems with finite FLF configurations must have the lower-triangular form (44). Not all paraxial systems can be constructed with one-lens arrangements, but they can by concatenation of up to three such subsystems [10].

4.3. The Brenner-Lohmann arrangement

Brenner and Lohmann [2] proposed the three-dimensional FLF arrangement shown in Fig. 5 in the x–z plane it is an imager while in the y–z plane it is a Fourier transformer. As we shall see in the second paper of this series, this arrangement can be used to produce the intensity image of the Wigner function of a one-dimensional signal.

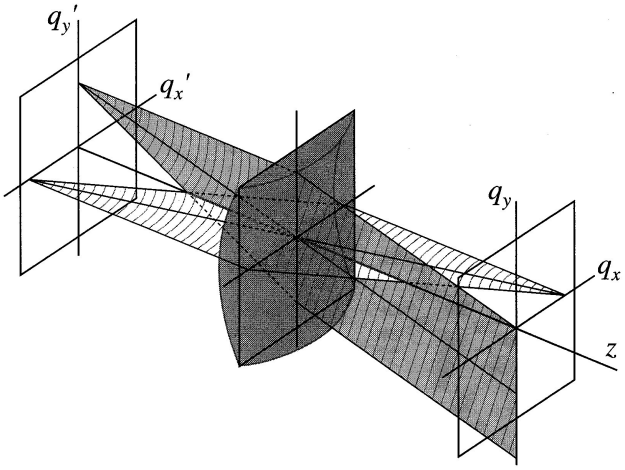

FIGURE 5. The Brenner-Lohmann optical system.

One places two fixed plane screens separated by $2z_o$ and, in the middle, two crossed cylindrical lenses, the imager in x with focal distance $f_x = \frac{1}{2}z_o = 1/g_x$ and the Fourier transformer in y with $f_y = z_o = 1/g_y$ (so $g_y = \frac{1}{2}g_x = 1/z_o$). One can use equivalently an axis-symmetric lens of power $g = 1/z_o$ glued to an x-cylindrical (the commonest anamorphotic lens element in Figure 5.) lens of the same power g, to obtain the same thin astigmatic lens $\mathcal{L}_{(2g,g)} = \mathcal{L}^{(x)}_{2g}\,\mathcal{L}^{(y)}_{g}$. Instead of using 4×4 matrices, we mark the commuting canonical transformations undergone separately in the x- and y-directions by separate 2×2 submatrices. The Brenner-Lohmann three-dimensional system $\mathcal{S}_{\rm BL} = \mathcal{T}_{z_o}\,\mathcal{L}_{(2g,g)}\,\mathcal{T}_{z_o}$ acts on paraxial monochromatic wavefields and separates in cartesian coordinates [Eqs. (29) and (30)],

$$
\begin{aligned}
(\mathcal{S}_{\rm BL}\bar{\psi})(q_x,q_y;k) &= e^{2ikz_o}\left[\mathcal{C}^{(x)}\begin{pmatrix} -1 & 0 \\ -kg & -1\end{pmatrix}\mathcal{C}^{(y)}\begin{pmatrix} 0 & 1/kg \\ -kg & 0\end{pmatrix}\bar{\psi}\right](q_x,q_y;k)\\
&= \frac{e^{ik/g}}{\sqrt{-2\pi i/kg}}\exp(i\tfrac{1}{2}kgq_x^2)\int_{\Re} dq'_y e^{-ikgq_yq'_y}\bar{\psi}(-q_x,q'_y;k) \qquad (48)\\
&= e^{ik/g}\,G_{-i/kg}(q_x)\,(\mathcal{F}_{\circ\mapsto kgq_y}\bar{\psi})(-q_x,\circ;k). \qquad (49)
\end{aligned}
$$

A photographic plate or charge-coupled-device camera does not measure the complex value of the wavefield $\bar{\psi}(\mathbf{q};k)$, but only its absolute square —the intensity of the wavefield, $|\bar{\psi}(\mathbf{q};k)|^2$. Thus, the phase contained in the factors $e^{ik/g}\,G_{-i/kg}(q_x)$ is immaterial to the measurement.

When the Brenner-Lohmann system is not quite 'in focus', but has extra free displacements z_1 and z_2 on the two sides of $\mathcal{S}_{\rm BL}$ in (49), then it works as

$$
\begin{aligned}
\mathcal{S}'_{\rm BL} = \mathcal{T}^k_{z_2}\mathcal{S}_{\rm BL}\mathcal{T}^k_{z_1} = \mathcal{T}_{z_o+z_2}\mathcal{L}_{(g,2g)}\mathcal{T}_{z_o+z_1} &= e^{ik(z_1+2z_o+z_2)}\\
&\times\begin{bmatrix} \mathcal{C}(x)\begin{pmatrix} -1-gz_2 & -(z_1+z_2+z_1z_2g)/k \\ -kg & -1-z_1g\end{pmatrix} & \mathbf{0} \\ \mathbf{0} & \mathcal{C}(y)\begin{pmatrix} -gz_2 & -z_1gz_2/k+1/kg \\ -kg & -z_1g\end{pmatrix}\end{bmatrix}. \qquad (50)
\end{aligned}
$$

The action along each coordinate can be understood by decomposing the real submatrices into their solvable and orthogonal factors,

$$
\begin{pmatrix} a & b \\ c & d\end{pmatrix} = \begin{pmatrix} 1 & 0 \\ -\gamma & 1\end{pmatrix}\begin{pmatrix} \mu & 0 \\ 0 & \mu^{-1}\end{pmatrix} \times\begin{pmatrix} \cos\beta & k^{-2}\sin\beta \\ -k^2\sin\beta & \cos\beta\end{pmatrix}, \qquad (51)
$$

with the solvable factor further decomposed into the lower-triangular matrix corresponding to a lens (multiplication by an oscillating Gaussian factor) and a diagonal matrix that contains the magnification factor. From elementary algebra, we obtain

$$
\mu = \sqrt{a^2+k^4b^2},\quad \begin{matrix}\sin\beta = k^2b/\mu,\\ \cos\beta = a/\mu,\end{matrix}\quad \gamma = -\frac{c}{a}-\frac{k^4b}{\mu^2 a}. \qquad (52)
$$

The leftmost factor in (51) does not modify the intensity in the unfocused Brenner-Lohmann system (50). The central factor entails magnifications for the x- and y- components, which for *small* z_1, z_2 can be approximated by the constant and linear terms in the Taylor series as follows:

$$
\begin{aligned}
\mu_x &= \sqrt{(1+gz_2)^2+k^2(z_1+z_2+z_1gz_2)^2} \approx 1+gz_2,\\
\mu_y &= \frac{k}{g}\sqrt{g^2z_2^2+k^2(1-z_1gz_2)^2/g^2} \approx \frac{k}{g}.
\end{aligned}
$$

This magnified wavefield is then the object of fractional Fourier transformation with angles β_x (to small unfocusing should correspond small β_x) and $\beta_y = \frac{1}{2}\pi + \beta'_y$ (small unfocusing of the Brenner-Lohmann system entails β'_y small). From (52) these Fourier angles are

$$
\beta_x \approx -k(z_1+z_2), \qquad \beta'_y \approx kz_2. \qquad (53)
$$

One of the most easiest aberrations to deal with mathematically is a simple error of focus. But even in this simple case, the assumption of the square aperture (rather than a circular aperture) is needed to keep the mathematics simple.

When a focusing error is presented, the center of curvature of a cylindrical wavefront converging toward the image of an object point-source lies either to the left or to the right of the image plane [12].

5. Conclusions

In this tutorial in paraxial wave optics we have presented the use of matrices for modelling different basic optical elements, such that a composite system is also represented by a matrix, given by the ordered product of the matrices that describe each of its components. These matrices turn out to be appropriate for the ray-optical description of the system, making the paraxial connection between ray and wave optics transparent.

A more general and perhaps more useful anamorphotic surface is the tones, of which the cylinder is a special case. The toric surface is found wherever anamorphotic optical system abound, from spectacle lenses to wide-screen cameras and projectors. Their treatment goes along the same lines as the cases already studied. Their quartic surfaces, and therefore to find the transfer equation a quartic polymorfal must be solved. Algebraic solution seems hardly worth the effort specially since numerical solutions are so easily available from high speed-computers [13].

The Brenner-Lohmann setup was presented here as a simple example of a paraxial optical system. The importance of this setup is that it allows the optical implementation of the Wigner function of a 1D signal, as will be described in the second part of this series of educational papers. There, we will define this function, summarize its properties, and explain the mathematical details of its production from the results presented here. We will also describe some practical aspects of the implementation of the setup in the lab, and compare the experimental results with those obtained from the theory.

Acknowledgements

The authors would like to thank Kurt B. Wolf for having unconditionally shared with us his vast knowledge and Neil Bruce (CCADET-UNAM) and Eugenio Ley Koo for the review of the text. C.J. Román had support from DGAPA-UNAM projects IN106595 and IN104597. Support of projects IN104198 *Optica Matemática* and 1N108900 *Detección Ultrarrápida y Ultrasensible* by the Dirección General de Asuntos del Personal Académico, UNAM, are gratefully acknowledged.

1. E. Wigner, On the quantum correction for thermodynamic equilibrium, *Phys. Rev.* **40** (1932) 749; J.E. Moyal, Quantum mechanics as a statistical theory, *Proc. Cambridge Philos. Soc.* **45** (1949) 99; J. W. Goodman, *Introduction to Fourier Optics*, McGraw-Hill (Electrical and Computer Engineering Series, 2nd Edition, 1996), chapter 2, p30.
2. H. Bartelt and K.-H. Brenner, The Wigner function an alternative signal representation in optics, *Israel J. Techn.* **18** (1980) 260; H.O. Bartelt, K.-H. Brenner and A. Lohmann, The Wigner distribution function and its optical production, *Opt. Comm.* **32** (1980) 32; K.-H. Brenner and A. H. Lohmann, Wigner distribution function display of complex 1D signals, *Opt. Comm.* **42** (1982) 310.
3. This distribution results from a uniformly-weighted superposition of plane waves traveling in the forward half sphere of directions, and interfering constructively at the image point.
4. R. Simon and K.B. Wolf, Structure of the set of paraxial optical systems, *Journal of the Optical Society of America A* **17** (2000) 342.
5. O. Castaños, E. López Moreno and K.B. Wolf, "Canonical transforms for paraxial wave optics." *Lie Methods in Optics*, J. Sánchez-Mondragón and K.B. Wolf, Eds., Lecture Notes in Physics, Vol. 250 (Springer Verlag, Heidelberg, 1986), Chapter 5, p. 159.
6. M. Moshinsky and C. Quesne, "Oscillator Systems," in *Proceedings of the 15th Solvay Conference in Physics (1970)* (Gordon and Breach, New York, 1974); *ibid.*, *J. Math. Phys* **12** (1971) 1772; *ibid.*, *J. Math. Phys* **12** (1971) 1780; M. Moshinsky, *SIAM J. Appl. Math.* **25** (1973) 193.
7. K.B. Wolf, *Integral Transforms in Science and Engineering* (Plenum Publ. Corp., New York, 1979), Chapters 9 and 10.
8. M. Born and E. Wolf, *Principles of Optics* (Cambridge University Press, Cambridge, 1999), 7th ed., p. 888.
9. H.M. Ozaktas, M.A. Kutay, and D. Mendlovic, *Advances in Imaging and Electron Physics*, edited by P.W. Hawkes (Academic Press, San Diego, 1999), Vol. 106, p. 239.
10. E.C.G. Sudarshan, N. Mukunda and R. Simon, *Opt. Acta* **32** (1985) 855; K.B. Wolf and G. Krötzsch, "El problema de las tres lentes," *Rev. Mex. Fís.* submitted (2000).
11. G.W. Forbes, V.I. Man'ko, H.M. Ozaktas, R. Simon, K.B. Wolf, *J. Opt. Soc. Am. A* **17** (2000) 2272.
12. J.W. Goodman, *Introduction to Fourier Optics* (McGraw-Hill, New York, 1996), 2nd ed., p. 148.
13. O.N. Stavroudis, *The Optics of Rays, Wavefronts and Caustics* (Academic Press, 1972), p. 95.